Mathematical Modelling and Analysis
Volume 25, Issue 4, 680–701, 2020
https://doi.org/10.3846/mma.2020.11692

http://mma.vgtu.lt
ISSN: 1392-6292
eISSN: 1648-3510

Numerical Solution of Variable-Order Time Fractional Weakly Singular Partial Integro-Differential Equations with Error Estimation

Haniye Dehestani[a], Yadollah Ordokhani[a] and Mohsen Razzaghi[b]

[a] *Department of Mathematics, Faculty of Mathematical Sciences, Alzahra University, Tehran, Iran*
[b] *Department of Mathematics and Statistics, Mississippi State University, Starkville, 39762 MS, USA*

E-mail(*corresp.*): ordokhani@alzahra.ac.ir
E-mail: h.dehestani@alzahra.ac.ir
E-mail: razzaghi@math.msstate.edu

Received December 10, 2019; revised September 4, 2020; accepted September 4, 2020

Abstract. In this paper, we apply Legendre-Laguerre functions (LLFs) and collocation method to obtain the approximate solution of variable-order time-fractional partial integro-differential equations (VO-TF-PIDEs) with the weakly singular kernel. For this purpose, we derive the pseudo-operational matrices with the use of the transformation matrix. The collocation method and pseudo-operational matrices transfer the problem to a system of algebraic equations. Also, the error analysis of the proposed method is given. We consider several examples to illustrate the proposed method is accurate.

Keywords: variable-order fractional partial integro-differential equations, weakly singular kernel, Legendre-Laguerre functions, pseudo-operational matrix.

AMS Subject Classification: 35R09; 65N35; 65L70.

1 Introduction

Partial integro-differential equations with a weakly singular kernel have numerous applications in mathematical physics and chemical reactions, such as the theory of elasticity, hydrodynamics, heat conduction, stereology [18] and the radiation of heat from semi-infinite solids [16]. Various numerical and analytical methods have been used for solving integro-differential equations. For example, Baleanu et al. [3] utilized the optimum q-homotopic analysis method for solving weakly singular kernel fractional fourth-order partial integro-differential equations, Tang [34] applied a finite difference scheme for partial integro-differential equations with a weakly singular kernel, McLean et al. [19] used Laplace transformation of an integro-differential equation of parabolic types, Nemati et al. [25] discussed the numerical solution of two-dimensional nonlinear Volterra integral equations by the Legendre polynomials, Fairweather [12] introduced spline collocation methods for a class of hyperbolic partial integro-differential equations, Dehestani et al. [9] proposed an efficient computational approach based on the Genocchi hybrid functions for solving a class of fractional Fredholm-Volterra functional integro-differential equations, Patel et al. [26] applied two-dimensional wavelets collocation scheme for linear and nonlinear Volterra weakly singular partial integro-differential equations and many other methods have been used in this type of equation, which can refer to [4, 10, 25, 30, 31, 32, 35].

In 1993, Samko and Ross [6], introduced an interesting generalization of fractional operators. They presented the study of fractional integration and differentiation when the order is not a constant but a function. Afterward, the variable order fractional calculus (VOFC) is presented as a useful tool with various applications in science and engineering, specifically, VOFC describes the mechanics of an oscillating mass subjected to a variable viscoelasticity damper and a linear spring [6] to characterize the dynamics of Van der Pol equation [11], to develop motion for spherical particle sedimentation in a quiescent viscous liquid [27], to analyze elastoplastic indentation problems [14], to interpolate the behavior of systems with multiple fractional terms [33] and to obtain variable-order fractional noise [29].

Several papers have been devoted to the study of variable-order fractional problems, such as variable-order fractional differential equations [17, 22, 24], variable-order fractional partial integro-differential equations [2, 8, 20, 21, 23] and so on. Limited work has been done in the study on VO-TF-PIDEs with the weakly singular kernel. Therefore, we consider the VO-TF-PIDEs with the weakly singular kernel as

$$D_t^{\gamma(x,t)}u(x,t)+\sum_{i=0}^{2}\sum_{j=0}^{2}\mu_{ij}\frac{\partial^{i+j}u(x,t)}{\partial x^i\partial t^j}=g(x,t)+\lambda\int_0^x\int_0^{h(t)}\frac{Gu(\xi,\eta)}{(x-\xi)^{\alpha}(t-\eta)^{\beta}}d\eta d\xi,$$
$$q-1<\gamma(x,t)\le q,\quad (x,t)\in[0,1]\times[0,\infty) \tag{1.1}$$

with initial conditions and boundary conditions

$$\begin{aligned} &u(x,0)=f_0(x), \quad \frac{\partial u(x,0)}{\partial t}=f_1(x),\\ &u(0,t)=\varphi_0(t), \quad u(1,t)=\varphi_1(t), \end{aligned} \tag{1.2}$$

where $\alpha,\beta\in[0,1)$, which are not both zero and $u(x,t)$ is an unknown function. The known functions $h(t)$, $f_0(x)$, $f_1(x)$, $\varphi_0(t)$ and $\varphi_1(t)$ are defined on interval

$\Omega = [0,1] \times [0,\infty)$, μ_{ij}, λ are real constants, q is a positive integer and G is an identity or differential operator. Also, $D_t^{\gamma(x,t)}$ denotes the variable order Caputo fractional derivative operator that is defined as follows [6, 8]:

$$D_t^{\gamma(x,t)} u(x,t) = \frac{1}{\Gamma(q-\gamma(x,t))} \int_0^t (t-s)^{q-\gamma(x,t)-1} \frac{\partial^q u(x,s)}{\partial s^q} ds,$$

for $q-1 < \gamma(x,t) \leq q$, $t > 0$ and $q \in Z^+$. To guarantee the existence and uniqueness of the solution of the proposed equation, we supposed that the functions $u(x,t)$ and $g(x,t)$ be sufficiently smooth functions. To solve this problem, we focus on providing a numerical scheme to solve VO-TF-PIDEs with the weakly singular kernel by LLFs and collocation method. Then, several numerical examples are presented to illustrate the effectiveness of the proposed method.

In modeling of physical phenomena, the variable order fractional derivatives are very powerful, because they have the memory with respect to time and spatial location. Therefore, the fractional derivatives statements in the proposed equation are replaced by the variable-order fractional derivative. Solving the problems by the variable-order fractional derivative with the help of an analytical method is not convenient. Hence, this fact motivates us to present the numerical algorithm base on Legendre-Laguerre functions. The Laguerre polynomials are orthogonal in the semi-infinite intervals which are appropriate for approximating problems of natural phenomena in semi-infinite intervals.

This paper is structured as follows. In Section 2, we introduce the formulation of LLFs and their properties. Section 3 is devoted to the pseudo-operational matrices of integration and variable-order fractional derivative for LLFs by use of the transformation matrix of Legendre and Laguerre polynomials to Taylor polynomials. In Section 5, we will describe a successful numerical approach, which is used for making up the solution. The convergence of the approximate solution is given in Section 6. In Section 7, we report our numerical results to demonstrate the accuracy of the proposed scheme. Also, conclusions are given in Section 8.

2 Legendre-Laguerre functions

In this section, we introduce two-dimensional LLFs, which obtain these functions with Legendre and Laguerre polynomials. Consider the shifted Legendre polynomials $P_m(x)$ on the interval $[0,1]$ as [7]

$$P_m(x) = \sum_{s=0}^{m} \frac{(-1)^{s+m}(m+s)!}{(m-s)!(s!)^2} x^s, \qquad m = 1, 2, 3, \ldots.$$

The shifted Legendre polynomials are orthogonal with respect to the weight function $w(x) = 1$ in the interval $[0,1]$ with the orthogonal property

$$\int_0^1 w(x) P_m(x) P_n(x) dx = \frac{1}{2m+1} \delta_{mn},$$

where δ_{mn} is the Kronecker function. The Laguerre polynomials $L_n(t)$ on the interval $[0,\infty)$ are defined as follows [7]:

$$L_n(t) = \sum_{k=0}^{n} \frac{(-1)^k n!}{(k!)^2(n-k)!} t^k, \quad n = 1,2,3,\dots. \tag{2.1}$$

The Laguerre polynomials are orthogonal with respect to the weight function $w(t) = e^{-t}$ in the interval $[0,\infty)$ with the orthogonal property

$$\int_0^\infty w(t) L_m(t) L_n(t) dt = \delta_{mn}.$$

Accordingly, we construct two-dimensional LLFs as follows:

$$\psi_{mn}(x,t) = P_m(x) L_n(t), \quad (x,t) \in \Omega, \quad m = 0,1,\dots,M, \quad n = 0,1,\dots,N.$$

Two-dimensional LLFs $\psi_{mn}(x,t)$, are the orthogonal basis with respect to the weight function $w(x,t) = e^{-t}$. Using the orthogonality property of Legendre and Laguerre polynomials, we obtain

$$\int_0^\infty \int_0^1 e^{-t} \psi_{mn}(x,t) \psi_{ij}(x,t) dx dt = \frac{1}{2m+1} \delta_{mi} \delta_{nj}.$$

A function $f(x,t)$, which is integrable in Ω, can be expanded as

$$f(x,t) = \sum_{m=0}^{\infty} \sum_{n=0}^{\infty} f_{mn} \psi_{mn}(x,t),$$
$$f_{mn} = (2m+1) \int_0^\infty \int_0^1 w(x,t) f(x,t) \psi_{mn}(x,t) dx dt.$$

Then, we have truncated series for f as

$$f(x,t) \simeq \sum_{m=0}^{M} \sum_{n=0}^{N} f_{mn} \psi_{mn}(x,t) = P^T(x) F L(t),$$

where

$$F = \left[\ f_{mn}\ \right]_{(M+1)\times(N+1)}, \quad m = 0,1,\dots,M, \quad n = 0,1,\dots,N,$$
$$P(x) = [P_0(x), P_1(x), \dots, P_M(x)]^T, \quad L(t) = [L_0(t), L_1(t), \dots, L_N(t)]^T.$$

3 Pseudo-operational matrices of integration for LLFs

In this section, we calculate the integral pseudo-operational matrix without coefficients and with the weakly singular coefficients for Legendre and Laguerre polynomials.

3.1 Pseudo-operational matrices of integration

To calculate the integral pseudo-operational matrices of Legendre polynomials, we use the Taylor polynomials $T_i(x) = x^i$, $i = 0, 1, \cdots, M$ [13]. The following relation holds among these polynomials and Legendre polynomials:

$$P(x) = D_1 T(x), \quad T(x) = [1, x, x^2, \ldots, x^M]^T,$$
$$D_1 = \left[d^1_{ij}\right], \quad d^1_{ij} = \begin{cases} \frac{(-1)^{i+j}(i+j)!}{(i-j)!(j!)^2}, & i \geq j, \\ 0, & otherwise, \end{cases} \qquad i, j = 0, 1, \ldots, M,$$

D_1 denotes the transformation matrix of the Legendre polynomials to the Taylor polynomials. Now, by integrating from $P(x)$, we obtain

$$\begin{aligned} \int_0^x P(\xi)d\xi &= \int_0^x D_1 T(\xi)d\xi = D_1 \int_0^x T(\xi)d\xi \\ &= xD_1H_1T(x) = xD_1H_1D_1^{-1}P(x) = xQ_1P(x), \end{aligned}$$

where $Q_1 = D_1H_1D_1^{-1}$ is an integral pseudo-operational matrix of Legendre polynomials and

$$H_1 = \left[h^1_{ij}\right], \qquad h^1_{ij} = \begin{cases} \frac{1}{i+1}, & i = j, \\ 0, & i \neq j, \end{cases} \qquad i, j = 0, 1, \ldots, M.$$

Moreover, to deal with the problem, we utilize the following integral

$$\begin{aligned} \int_0^x \xi P(\xi)d\xi &= \int_0^x \xi D_1 T(\xi)d\xi = D_1 \int_0^x \xi T(\xi)d\xi \\ &= x^2 D_1 \hat{H}_1 T(x) = x^2 D_1 \hat{H}_1 D_1^{-1} P(x) = x^2 \hat{Q}_1 P(x), \end{aligned}$$

where $\hat{Q}_1 = D_1 \hat{H}_1 D_1^{-1}$ and

$$\hat{H}_1 = \left[\hat{h}^1_{ij}\right], \quad \hat{h}^1_{ij} = \begin{cases} 1/(i+2), & i = j, \\ 0, & i \neq j, \end{cases} \qquad i, j = 0, 1, \ldots, M.$$

Moreover, we can write $L(t)$ in the matrix form as follows:

$$L(t) = D_2 T(t), \quad T(t) = [1, t, t^2, \ldots, t^N]^T,$$
$$D_2 = [d^2_{ij}]_{(N+1)\times(N+1)}, \quad d^2_{ij} = \begin{cases} \frac{(-1)^j (i)!}{(i-j)!(j!)^2}, & i \geq j, \\ 0, & \text{otherwise}, \end{cases} \qquad i, j = 0, 1, \ldots, N,$$

D_2 is the transformation matrix of the Laguerre polynomials to the Taylor polynomials. Then, by integrating $L(t)$ on interval $[0, h(t)]$, we have

$$\begin{aligned} \int_0^{h(t)} L(\eta)d\eta &= \int_0^{h(t)} D_2 T(\eta)d\eta = D_2 \int_0^{h(t)} T(\eta)d\eta = h(t) D_2 H_2 T(h(t)) \\ &= h(t) D_2 H_2 D_2^{-1} L(h(t)) = h(t) Q_2 L(h(t)), \end{aligned} \tag{3.1}$$

where $Q_2 = D_2H_2D_2^{-1}$ and

$$H_2 = \left[h^2_{ij}\right], \quad h^2_{ij} = \begin{cases} 1/(i+1), & i = j, \\ 0, & i \neq j, \end{cases} \qquad i, j = 0, 1, \ldots, N.$$

In Equation (3.1), by putting $h(t)=t$, we have $\int_0^t L(\eta)d\eta = tQ_2L(t)$, where we introduce Q_2 as an integral pseudo-operational matrix of Laguerre polynomials. In addition, we need

$$\int_0^t \eta L(\eta)d\eta = \int_0^t \eta D_2T(\eta)d\eta = D_2\int_0^t \eta T(\eta)d\eta$$
$$= t^2D_2\hat{H}_2T(t) = t^2D_2\hat{H}_2D_2^{-1}L(t) = t^2\hat{Q}_2L(t), \quad \hat{Q}_2 = D_2\hat{H}_2D_2^{-1},$$

where

$$\hat{H}_2 = \left[\hat{h}_{ij}^2\right], \quad \hat{h}_{ij}^2 = \begin{cases} \frac{1}{i+2}, & i=j, \\ 0, & i\neq j, \end{cases} \qquad i,j=0,1,\ldots,N.$$

3.2 Pseudo-operational matrix with the weakly singular coefficients

To deal with an integral part of Equation (1.1), we present the pseudo-operational matrix with the weakly singular coefficients. Hence, we obtain integral of Legendre polynomials with the weakly singular kernel $\frac{1}{(x-\xi)^\alpha}$:

$$\begin{aligned}\int_0^x \frac{P(\xi)}{(x-\xi)^\alpha}d\xi &= \int_0^x \frac{D_1T(\xi)}{(x-\xi)^\alpha}d\xi = D_1\int_0^x \frac{T(\xi)}{(x-\xi)^\alpha}d\xi \\ &= x^{1-\alpha}D_1S_1T(x) = x^{1-\alpha}D_1S_1D_1^{-1}P(x) = x^{1-\alpha}\tilde{S}_1P(x),\end{aligned}$$

where $\tilde{S}_1 = D_1S_1D_1^{-1}$ is the pseudo-operational matrix with the weakly singular coefficients for Legendre polynomials and

$$S_1 = \left[s_{ij}^1\right], \quad s_{ij}^1 = \begin{cases} \frac{\Gamma(1-\alpha)\Gamma(1+i)}{\Gamma(2+i-\alpha)}, & i=j, \\ 0, & i\neq j, \end{cases} \qquad i,j=0,1,\ldots,M.$$

Also, we obtain integration of Laguerre polynomials with the weakly singular kernel $1/(t-\eta)^\beta$ on interval $[0,h(t)]$ as:

$$\int_0^{h(t)} \frac{L(\eta)}{(t-\eta)^\beta}d\eta = \int_0^{h(t)} \frac{D_2T(\eta)}{(t-\eta)^\beta}d\eta = D_2\int_0^{h(t)} \frac{T(\eta)}{(t-\eta)^\beta}d\eta$$
$$= h(t)^{1-\beta}D_2S_2T(h(t)) = h(t)^{1-\beta}D_2S_2D_2^{-1}L(h(t)) = h(t)^{1-\beta}\tilde{S}_2L(h(t)),$$

where $\tilde{S}_2 = D_2S_2D_2^{-1}$ the pseudo-operational matrix with the weakly singular coefficients for Laguerre polynomials and

$$S_2 = \left[s_{ij}^2\right], \quad s_{ij}^2 = \begin{cases} \frac{\Gamma(1-\beta)\Gamma(1+i)}{\Gamma(2+i-\beta)}, & i=j, \\ 0, & i\neq j, \end{cases} \qquad i,j=0,1,\ldots,N.$$

4 Pseudo-operational matrix of the variable-order fractional derivative

In this section, we derive the pseudo-operational matrix of the variable-order fractional derivative of Laguerre polynomials by using some properties of Caputo variable-order fractional derivative.

Theorem 1. *The pseudo-operational matrix of the variable-order fractional derivative of order $q-1<\gamma(x,t)\leq q$ for the Laguerre polynomials is given by*

$$D_t^{\gamma(x,t)}L(t)\simeq t^{q-\gamma(x,t)}\xi_N^{\gamma(x,t)}L(t),$$

where $\xi_N^{\gamma(x,t)}$ is called the pseudo-operational matrix of variable-order fractional derivative for the Laguerre polynomials.

Proof. By using some properties of Caputo variable-order fractional derivative and Equation (2.1), we obtain

$$\begin{aligned}D_t^{\gamma(x,t)}L_n(t)&=D_t^{\gamma(x,t)}\Big(\sum_{k=0}^{n}\frac{(-1)^k n!}{(k!)^2(n-k)!}t^k\Big)=\sum_{k=0}^{n}\frac{(-1)^k n!}{(k!)^2(n-k)!}D_t^{\gamma(x,t)}(t^k)\\&=\sum_{k=0}^{n}\frac{(-1)^k n!}{(k!)^2(n-k)!}\frac{\Gamma(k+1)}{\Gamma(k-\gamma(x,t)+1)}t^{k-\gamma(x,t)}\\&=t^{q-\gamma(x,t)}\sum_{k=q}^{n}b_{n,k}^{\gamma(x,t)}t^{k-q},\qquad b_{n,k}^{\gamma(x,t)}=\frac{(-1)^k n!\Gamma(k+1)}{(k!)^2(n-k)!\Gamma(k-\gamma(x,t)+1)}.\end{aligned}$$

Now, we approximate t^{k-q} by $N+1$ terms of Laguerre polynomials $t^{k-q}\simeq\sum_{j=0}^{N}c_{k,j}L_j(t)$. By employing the above equations, we get

$$\begin{aligned}D_t^{\gamma(x,t)}L_n(t)&\simeq t^{q-\gamma(x,t)}\sum_{k=q}^{n}b_{n,k}^{\gamma(x,t)}\sum_{j=0}^{N}c_{k,j}L_j(t)=t^{q-\gamma(x,t)}\sum_{j=0}^{N}\Big(\sum_{k=q}^{n}\theta_{n,k,j}^{\gamma(x,t)}\Big)L_j(t)\\&=t^{q-\gamma(x,t)}\sum_{j=0}^{N}\xi_{n,k,j}^{\gamma(x,t)}L_j(t),\qquad \theta_{n,k,j}^{\gamma(x,t)}=b_{n,k}^{\gamma(x,t)}c_{k,j}.\end{aligned}\tag{4.1}$$

The matrix form of Equation (4.1) can be written as follows:

$$D_t^{\gamma(x,t)}L_n(t)\simeq t^{q-\gamma(x,t)}\begin{bmatrix}\sum_{k=q}^{n}\theta_{n,k,0}^{\gamma(x,t)} & \sum_{k=q}^{n}\theta_{n,k,1}^{\gamma(x,t)} & \cdots & \sum_{k=q}^{n}\theta_{n,k,N}^{\gamma(x,t)}\end{bmatrix}L(t).$$

□

Also, according to the above process, we obtain

$$D_t^{\gamma(x,t)}(tL(t))\simeq t^{1+q-\gamma(x,t)}\hat{\xi}_N^{\gamma(x,t)}L(t),$$

where $\hat{\xi}_N^{\gamma(x,t)}$ similar $\xi_N^{\gamma(x,t)}$ is calculated.

5 Description of the method

In this section, we present the numerical scheme for solving the problem given in Equation (1.1) with conditions in Equation (1.2). According to the proposed equation, we expand the following function by the LLFs as:

$$\frac{\partial^4 u(x,t)}{\partial x^2\partial t^2}\simeq P^T(x)UL(t),\tag{5.1}$$

where $U_{(M+1)\times(N+1)}$ is an unknown matrix as

$$U = [u_{mn}]_{(M+1)\times(N+1)}, \quad m = 0, 1, \dots, M, \quad n = 0, 1, \dots, N.$$

To approximate the other functions, we use the pseudo-operational matrices that presented in previous sections. By integrating the above equation with respect to t and substituting initial conditions into it, we obtain

$$\frac{\partial^3 u(x,t)}{\partial x^2 \partial t} \simeq tP^T(x)UQ_2L(t) + f_1''(x), \tag{5.2}$$

$$\frac{\partial^2 u(x,t)}{\partial x^2} \simeq t^2 P^T(x)UQ_2\hat{Q}_2L(t) + tf_1''(x) + f_0''(x). \tag{5.3}$$

Now by integrating Equation (5.3) of order 2 with respect to x, we get

$$\frac{\partial u(x,t)}{\partial x} \simeq xt^2 P^T(x)Q_1^T UQ_2\hat{Q}_2L(t) + t(f_1'(x) - f_1'(0)) + (f_0'(x) - f_0'(0)) + \frac{\partial u(0,t)}{\partial x}, \tag{5.4}$$

$$\begin{aligned} u(x,t) \simeq\ & x^2t^2 P^T(x)\hat{Q}_1^T Q_1^T UQ_2\hat{Q}_2L(t) + t(f_1(x) - f_1(0) - xf_1'(0)) \\ & + (f_0(x) - f_0(0) - xf_0'(0)) + x\frac{\partial u(0,t)}{\partial x} + \varphi_0(t). \end{aligned} \tag{5.5}$$

Function $\frac{\partial u(0,t)}{\partial x}$ is unknown, in order to obtain this function, integrating Equation (5.4) with respect to x from 0 to 1

$$\begin{aligned} u(1,t) - u(0,t) \simeq\ & t^2 \left(\int_0^1 xP^T(x)dx \right) Q_1^T UQ_2\hat{Q}_2L(t) + t(f_1(1) - f_1(0) - f_1'(0)) \\ & + (f_0(1) - f_0(0) - f_0'(0)) + \frac{\partial u(0,t)}{\partial x}, \end{aligned}$$

where

$$\int_0^1 xP^T(x)dx = \int_0^1 xT^T(x)D_1^T dx = S^T D_1^T, \quad S = \left[\frac{1}{2}, \frac{1}{3}, \frac{1}{4}, \dots, \frac{1}{M+2} \right]^T.$$

Then,

$$\begin{aligned} \frac{\partial u(0,t)}{\partial x} \simeq\ & \varphi_1(t) - \varphi_0(t) - t^2 S^T D_1^T Q_1^T UQ_2\hat{Q}_2L(t) - t(f_1(1) - f_1(0) - f_1'(0)) \\ & - (f_0(1) - f_0(0) - f_0'(0)). \end{aligned}$$

Also, we need to calculate the following expression. By integrating Equation (5.1) of order 2 with respect to x and using the boundary conditions, we have

$$\frac{\partial^3 u(x,t)}{\partial x \partial t^2} \simeq xP^T(x)Q_1^T UL(t) + \frac{\partial^3 u(0,t)}{\partial x \partial t^2}, \tag{5.6}$$

$$\frac{\partial^2 u(x,t)}{\partial t^2} \simeq x^2 P^T(x)\hat{Q}_1^T Q_1^T UL(t) + x\frac{\partial^3 u(0,t)}{\partial x \partial t^2} + \varphi_0''(t). \tag{5.7}$$

In Equations (5.6) and (5.7), $\frac{\partial^3 u(0,t)}{\partial x \partial t^2}$ is an unknown function. By integrating Equation (5.6) from 0 to 1 with respect to x, we get

$$\frac{\partial^3 u(0,t)}{\partial x \partial t^2} \simeq \varphi_1''(t) - \varphi_0''(t) - S^T D_1^T Q_1^T U L(t).$$

By integrating Equation (5.7) with respect to t, we have

$$\begin{aligned}\frac{\partial u(x,t)}{\partial t} \simeq & x^2 t P^T(x) \hat{Q}_1^T Q_1^T U Q_2 L(t) + x(\varphi_1'(t) - \varphi_0'(t) - t S^T D_1^T Q_1^T U Q_2 L(t)) \\ & + \varphi_0'(t) + f_1(x).\end{aligned}$$

In addition, we calculate the variable-order fractional derivatives by applying the pseudo-operational matrix presented in Section 4. Therefore, we achieve

$$\begin{aligned}D_t^{\gamma(x,t)} u(x,t) \simeq & \, x^2 t^{2+q-\gamma(x,t)} P^T(x) \hat{Q}_1^T Q_1^T U Q_2 \hat{Q}_2 \bar{\xi}_N^{\gamma(x,t)} L(t) \\ & + \frac{\Gamma(2)}{\Gamma(2-\gamma(x,t))} t^{1-\gamma(x,t)} (f_1(x) - f_1(0) - x f_1'(0)) \\ & + x(D_t^{\gamma(x,t)} \varphi_1(t) - D_t^{\gamma(x,t)} \varphi_0(t) - t^{2+q-\gamma(x,t)} S^T D_1^T Q_1^T U Q_2 \hat{Q}_2 \bar{\xi}_N^{\gamma(x,t)} L(t) \\ & - \frac{\Gamma(2)}{\Gamma(2-\gamma(x,t))} t^{1-\gamma(x,t)} (f_1(1) - f_1(0) - f_1'(0))) + D_t^{\gamma(x,t)} \varphi_0(t),\end{aligned}$$

so that $\bar{\xi}_N^{\gamma(x,t)}$ according to the process in Theorem 1 is obtained. Consequently, by using the pseudo-operational matrix and following integration formula

$$\int_0^x \frac{\xi^n}{(x-\xi)^\alpha} d\xi = \frac{\Gamma(1-\alpha)\Gamma(1+n)}{\Gamma(2-\alpha-n)} x^{1-\alpha+n},$$

we approximate an integral part of Equation (1.1). In specific example

$$\begin{aligned}\int_0^x \int_0^t \frac{u_{t^2}(\xi,\eta)}{(x-\xi)^{\frac{1}{2}}} d\eta d\xi \simeq & \int_0^x \frac{P^T(\xi)}{(x-\xi)^{\frac{1}{2}}} d\xi U Q_2 \hat{Q}_2 \int_0^t \eta^2 L(\eta) d\eta \\ & + \int_0^x \int_0^t \frac{\eta f_1''(\xi)}{(x-\xi)^{\frac{1}{2}}} d\xi d\eta + \int_0^x \int_0^t \frac{f_0''(\xi)}{(x-\xi)^{\frac{1}{2}}} d\xi d\eta \\ & \simeq x^{\frac{1}{2}} t^3 P^T(x) \tilde{S}_1^T U Q_2 \hat{Q}_2 \tilde{Q}_2 L(T) + \frac{t^2}{2} \int_0^x \frac{f_1''(\xi)}{(x-\xi)^{\frac{1}{2}}} d\xi + t \int_0^x \frac{f_0''(\xi)}{(x-\xi)^{\frac{1}{2}}} d\xi\end{aligned}$$

and

$$\begin{aligned}\int_0^x \int_0^t \frac{u_{x^2}(\xi,\eta)}{(t-\eta)^{\frac{1}{2}}} d\eta d\xi \simeq & \int_0^x \xi^2 P^T(\xi) d\xi \hat{Q}_2^T Q_2^T U \int_0^t \frac{L(\eta)}{(t-\eta)^{\frac{1}{2}}} d\eta \\ & + \frac{x^2}{2} \int_0^t \frac{\varphi_1''(\eta) - \varphi_0''(\eta)}{(t-\eta)^{\frac{1}{2}}} d\eta - \frac{x^2}{2} S^T D_1^T Q_1^T U \int_0^t \frac{L(\eta)}{(t-\eta)^{\frac{1}{2}}} d\eta \\ + x \int_0^t \frac{\varphi_0''(\eta)}{(t-\eta)^{\frac{1}{2}}} d\eta \simeq & \, x^3 t^{\frac{1}{2}} P^T(x) \tilde{Q}_1^T \hat{Q}_1^T Q_1^T U \tilde{S}_2 L(t) + \frac{x^2}{2} \int_0^t \frac{\varphi_1''(\eta) - \varphi_0''(\eta)}{(t-\eta)^{\frac{1}{2}}} d\eta \\ & - \frac{1}{2} x^2 t^{\frac{1}{2}} S^T D_1^T Q_1^T U \tilde{S}_2 L(t) + x \int_0^t \frac{\varphi_0''(\eta)}{(t-\eta)^{\frac{1}{2}}} d\eta.\end{aligned}$$

$\tilde{Q}_1$ and $\tilde{Q}_2$ similar to $\hat{Q}_1$ and $\hat{Q}_2$ are calculated, respectively. So that,

$$\int_0^x \xi^2 P(\xi)d\xi = x^3\tilde{Q}_1 P(x), \quad \int_0^t \eta^2 L(\eta)d\eta = t^3\tilde{Q}_2 L(t),$$

where $\tilde{Q}_1 = D_1\tilde{H}_1 D_1^{-1}$, $\tilde{Q}_2 = D_2\tilde{H}_2 D_2^{-1}$ and

$$\tilde{H}_1 = \left[\tilde{h}^1_{ij}\right], \quad \tilde{h}^1_{ij} = \begin{cases} 1/(i+3), & i=j, \\ 0, & i\neq j, \end{cases} \qquad i,j=0,1,\ldots,M,$$
$$\tilde{H}_2 = \left[\tilde{h}^2_{ij}\right], \quad \tilde{h}^2_{ij} = \begin{cases} 1/(i+3), & i=j, \\ 0, & i\neq j, \end{cases} \qquad i,j=0,1,\ldots,N.$$

We obtain an algebraic equation by substituting the above approximate functions in Equation (1.1). Then, we collocated this equation in nodal points of Newton-Cotes [7]. Ultimately, we get an unknown matrix U by solving a system of algebraic equations and using Newton's iterative method. Finally, by substituting U in Equation (5.5), we achieve the approximate solution to the problem.

6 Convergence and error estimation

In this section, we present the upper bound of errors by the following theorem in Sobolev space [5]. For this goal, the Sobolev norm of integer order $\mu \geq 0$ on the interval (a,b) in $\mathbb{R}$ is defined as

$$\|f\|_{H^\mu(a,b)} = \left(\sum_{j=0}^{\mu} \|f^{(j)}\|^2_{L^2(a,b)}\right)^{\frac{1}{2}}.$$

The seminorm is defined as [5]

$$|f|_{H^{\mu;M}(a,b)} = \left(\sum_{j=\min(\mu,M+1)}^{\mu} \|f^{(j)}\|^2_{L^2(a,b)}\right)^{\frac{1}{2}}.$$

Lemma 1. *Let $f\in H^\mu(0,1)$, such that $P_M f = \sum_{m=0}^{M} f_m P_m$ is the best approximation of f, then for $1\leq k\leq \mu$, we get*

$$\|f - P_M f\|_{H^k(0,1)} \leq CM^{2k-\frac{1}{2}-\mu}|f|_{H^{\mu;M}(0,1)},$$

where C depends on μ.

Also, Laguerre approximations in weighted Sobolev spaces on the half-line $\mathbb{R}_+$ of integer order $\mu\geq 0$ is defined as follows:

$$\|g\|_{H^\mu(\mathbb{R}_+)} = \left(\sum_{j=0}^{\mu} \|g^{(j)}\|^2_{L^2_w(\mathbb{R}_+)}\right)^{\frac{1}{2}}, \qquad \|g\|^2_{L^2_w(\mathbb{R}_+)} = \left(\int_{\mathbb{R}_+} g^2(t)e^{-t}dt\right)^{\frac{1}{2}}.$$

Lemma 2. *Let $g \in H^{\mu}(\mathbb{R}_+)$, such that $P_N g = \sum_{n=0}^{N} g_n L_n$ is the best approximation of g then for any $\mu \geq 0$ and $0 \leq r \leq \mu$, we have [5]*

$$\|g - P_N g\|_{H^k(\mathbb{R}_+)} \leq C N^{r-\frac{\mu}{2}} \|g\|_{H^{\mu}_{w,\mu}(\mathbb{R}_+)},$$

where C depends on μ.

Theorem 2. *Suppose that u_M and u_N are approximated with truncated Legendre-Laguerre series u_{Mn} and u_{mN}, respectively. So that,*

$$u_{Mn}(x,t) = \sum_{n=0}^{N} a_{Mn} P_M(x) L_n(t), \quad u_M(x,t) = \sum_{n=0}^{\infty} a_{Mn} P_M(x) L_n(t),$$
$$u_{mN}(x,t) = \sum_{m=0}^{M} a_{mN} P_m(x) L_N(t), \quad u_N(x,t) = \sum_{m=0}^{\infty} a_{mN} P_m(x) L_N(t).$$

Then, the following estimates hold

$$\|u_M - u_{Mn}\|_{H^k_w(\Omega)} \leq C N^{r-\frac{\mu}{2}} \|u_M\|_{H^{\mu}_{w,\mu-1}(\mathbb{R}_+)} \|P_M\|_{H^k_w[0,1]},$$
$$\|u_N - u_{mN}\|_{H^k_w(\Omega)} \leq C M^{2k-\frac{1}{2}-\mu} |u_N|_{H^{\mu}_{w,\mu-1}[0,1]} \|L_N\|_{H^k_w(\mathbb{R}_+)}.$$

Proof. According to the hypothesizes and Lemmas 1 and 2, we have

$$\begin{aligned}
\|u_M - u_{Mn}\|_{H^k_w(\Omega)} &= \| \sum_{n=0}^{\infty} a_{Mn} P_M L_n - \sum_{n=0}^{N} a_{Mn} P_M L_n \|_{H^k_w(\Omega)} \\
&\leq \| \sum_{n=0}^{\infty} a_{Mn} L_n - \sum_{n=0}^{N} a_{Mn} L_n \|_{H^k_w(\mathbb{R}_+)} \|P_M\|_{H^k_w[0,1]} \\
&\leq C N^{r-\frac{\mu}{2}} \|u_M\|_{H^{\mu}_{w,\mu-1}(\mathbb{R}_+)} \|P_M\|_{H^k_w[0,1]}.
\end{aligned}$$

And also,

$$\begin{aligned}
\|u_N - u_{mN}\|_{H^k_w(\Omega)} &= \| \sum_{m=0}^{\infty} u_{mN} P_m L_N - \sum_{m=0}^{M} u_{mN} P_m L_N \|_{H^k_w(\Omega)} \\
&\leq \| \sum_{m=0}^{\infty} u_{mN} P_m - \sum_{m=0}^{M} u_{mN} P_m \|_{H^k_w[0,1]} \|L_N\|_{H^k_w(\mathbb{R}_+)} \\
&\leq C M^{2k-\frac{1}{2}-\mu} |u_N|_{H^{\mu,M}[0,1]} \|L_N\|_{H^k_w(\mathbb{R}_+)}.
\end{aligned}$$

Hence, we obtain the upper bound of the errors. □

Corollary 1. Suppose $u_N, u_M \in H_{\mu}(\Omega)$ and $\mu \geq 1$ then by setting $N, M \geq \mu - 1$, and considering the previous theorem, we deduce

$$\|u_M - u_{Mn}\|_{H^k_w(\Omega)} \leq C N^{r-\frac{\mu}{2}} \|u_M\|_{H^{\mu}_{w,\mu-1}(\mathbb{R}_+)} \|P_M\|_{H^k_w[0,1]},$$
$$\|u_N - u_{mN}\|_{H^k_w(\Omega)} \leq C M^{2k-\frac{1}{2}-\mu} \|u_N^{(\mu)}\|_{L^2[0,1]} \|L_N\|_{H^k_w(\mathbb{R}_+)}.$$

In the first and second inequality, the values of M and N are constant, respectively. According to this fact, in the first inequality, the rate of convergence of u_{Mn} to u_M is faster than $\frac{1}{N}$ to the power of $\frac{N}{2}+\frac{1}{2}-r$. And also, in the second inequality, the rate of convergence of u_{mN} to u_N is faster than $\frac{1}{M}$ to the power of $M-2k+\frac{3}{2}$.

7 Illustrative examples

In order to test the validity of the present method, we consider some examples and apply the technique in Section 5 for solving them. Then, the numerical results are compared with their exact solution and other methods. The computations were performed on a personal computer and the codes were written in MATLAB 2016.

Example 1. Consider VO-TF-PIDEs with weakly singular kernel [30]

$$D_t^{\gamma(x,t)}u(x,t) = u(x,t) + g(x,t) + \int_0^x \int_0^{h(t)} \frac{u_{t^2}(\xi,\eta)}{(x-\xi)^{\frac{1}{2}}} d\eta d\xi, \qquad 0 < \gamma(x,t) \le 1$$

with initial conditions $u(x,0)=0$, $\frac{\partial u(x,0)}{\partial t}=0$, $0 \le x \le 1, t > 0$, where $g(x,t) = \frac{\Gamma(3)}{\Gamma(3-\gamma(x,t))}xt^{2-\gamma(x,t)} - xt^2 - \frac{8}{3}x^{\frac{3}{2}}h(t)$. The exact solution of this example is $u(x,t)=xt^2$. To evaluate the precision of the proposed method, we present the norm of residual error

$$\|Res_{MN}\|_{2,w}^2 = \int_0^1 \int_0^\infty Res_{MN}^2(x,t)w(x,t)dxdt,$$

where

$$\begin{aligned} Res_{MN}(x,t) =& t^{3-\gamma(x,t)}P^T(x)UQ_2\hat{Q}_2\bar{\xi}_N^{\gamma(x,t)}L(t) - t^2P^T(x)UQ_2\hat{Q}_2L(t) \\ &- g(x,t) - x^{\frac{1}{2}}h(t)P^T(x)\tilde{S}_1^TUQ_2L(h(t)). \end{aligned}$$

By taking $M=N=1, h(t)=\cos(t), \gamma(x,t)=1$ and $M=N=1, h(t)=t, \gamma(x,t)=1-0.5\exp(-xt)$, we get respectively

$$\|Res_{11}\|_{2,w}^2 = 6.5274 \times 10^{-32}, \quad \|Res_{11}\|_{2,w}^2 = 1.7231 \times 10^{-31}.$$

In Table 1, the absolute errors are obtained between the approximate solutions and the exact solution using Legendre-Laguerre functions for various functions of $h(t)$ and $\gamma(x,t)$ with $M=N=1$ (here $\gamma_3(x,t)=0.8+0.005\cos(xt)$). Also, maximum absolute errors with various functions of $h(t)$ and $\gamma(x,t)$ for $x=1$ and $t \in [0,20]$ with $M=N=1$ and CPU time (in seconds) are shown in Table 2. Due to the errors in figure [30], the proposed method is more accurate in comparison to the method in [30] with $h(t)=t$, $N=2$ and $\gamma(x,t)=1$.

Example 2. Consider VO-TF-PIDEs with weakly singular kernel

$$D_{t^2}^{\gamma(x,t)}u(x,t) = u(x,t) + \frac{\partial u}{\partial x}(x,t) + g(x,t) + \int_0^x \int_0^{h(t)} \frac{u_{xt^2}(\xi,\eta)}{(x-\xi)^{\frac{1}{4}}} d\eta d\xi,$$

Table 1. Absolute errors for various functions of $h(t)$ and $\gamma(x,t)$ with $M=1, N=1$ of Example 1.

(x_i,t_i)	$\gamma(x,t)=1$		$\gamma(x,t)=0.875$		$\gamma_3(x,t)$
	$h(t)=t$	$h(t)=\exp(t^2)$	$h(t)=t$	$h(t)=\exp(t^2)$	$h(t)=t$
0	0	0	0	0	0
$(0.1,0.1)$	2.44×10^{-18}	1.67×10^{-18}	2.62×10^{-19}	1.04×10^{-18}	8.99×10^{-20}
$(0.2,0.2)$	9.85×10^{-18}	6.03×10^{-18}	1.57×10^{-18}	3.72×10^{-18}	7.74×10^{-19}
$(0.3,0.3)$	2.22×10^{-17}	1.21×10^{-17}	4.64×10^{-18}	7.42×10^{-18}	2.61×10^{-18}
$(0.4,0.4)$	3.96×10^{-17}	1.92×10^{-17}	1.00×10^{-17}	1.15×10^{-17}	6.09×10^{-18}
$(0.5,0.5)$	6.17×10^{-17}	2.64×10^{-17}	1.82×10^{-17}	1.57×10^{-17}	1.15×10^{-17}
$(0.6,0.6)$	8.85×10^{-17}	3.33×10^{-17}	2.95×10^{-17}	1.93×10^{-17}	1.93×10^{-17}
$(0.7,0.7)$	1.19×10^{-16}	3.91×10^{-17}	4.41×10^{-17}	2.21×10^{-17}	2.95×10^{-17}
$(0.8,0.8)$	1.54×10^{-16}	4.34×10^{-17}	6.22×10^{-17}	2.39×10^{-17}	4.22×10^{-17}
$(0.9,0.9)$	1.92×10^{-16}	4.60×10^{-17}	8.36×10^{-17}	2.42×10^{-17}	5.76×10^{-17}
$(1,1)$	2.33×10^{-16}	4.64×10^{-17}	1.08×10^{-16}	2.30×10^{-17}	7.54×10^{-17}

Table 2. Maximum absolute errors for various functions of $h(t), \gamma(x,t)$ for $x=1, t\in[0,20]$ with $N=M=1$ of Example 1.

$h(t)$	$\gamma(x,t)$	Maximum absolute error	CPU
t	1	5.4665×10^{-14}	9.9919×10^{-2}
	0.5	2.3149×10^{-12}	1.0213×10^{-1}
	$1-\exp(-xt)$	2.2154×10^{-12}	1.0622×10^{-1}
$\cos(t)$	1	5.9807×10^{-14}	1.0682×10^{-1}
	0.5	3.1643×10^{-12}	1.0680×10^{-1}
	$1-\exp(-xt)$	3.7712×10^{-12}	1.1115×10^{-1}

$1<\gamma(x,t)\le 2$, with initial conditions $u(x,0)=-x$, $\frac{\partial u(x,0)}{\partial t}=0$, $0\le x\le 1$, and boundary conditions $u(0,t)=0$, $u(1,t)=t^3-1$, $t>0$, with $g(x,t)=\frac{6xt^{3-\gamma(x,t)}}{\Gamma(4-\gamma(x,t))}-\frac{2}{3}x^{\frac{3}{4}}h(t)^2-x(t^3-1)-t^3+1$. The exact solution of this example is $u(x,t)=x(t^3-1)$. By applying the proposed method with $M=1, N=3$ and various functions $h(t)=t, \sin(t), \cos(t), t^2+1$ and $\gamma(x,t)=1.25, 1.5, 1.75, 2-0.2\exp(-xt)$, we achieved the exact solution.

Example 3. Consider the following VO-TF-PIDEs with weakly singular kernel

$$\frac{\partial u}{\partial t}(x,t)+D_t^{\gamma(x,t)}u(x,t)=-\frac{\partial u}{\partial x}(x,t)+\frac{\partial^2 u}{\partial x^2}(x,t)+g(x,t)$$
$$+\lambda\int_0^x\int_0^{h(t)}\frac{u(\xi,\eta)}{(x-\xi)^{\frac{1}{2}}}d\eta d\xi,$$

$0<\gamma(x,t)\le 1$, with initial condition $u(x,0)=10x^2(1-x)^2$, $0\le x\le 1$ and boundary conditions $u(0,t)=u(1,t)=0$, $t>0$, with $g(x,t)=10(1+\frac{t^{2-\gamma(x,t)}}{\Gamma(2-\gamma(x,t))})x^2(1-x)^2-\frac{16}{63}\lambda h(t)x^{\frac{5}{2}}(t+2)(16x^2-36x+21)+10(4x^3-6x^2+2x-12x^2+12x-2)(t+1)$. The exact solution of this example is $u(x,t)=10(t+1)x^2(1-x)^2$. Considering $\lambda=0$, we have a variable order time-fractional mobile-immobile advection-dispersion equations. Recently, many papers have published that aim to provide the satisfactory results of these equations. variable order time-fractional mobile-immobile advection-dispersion model, which is appeared to simulate solute transport in watershed catchments and rivers. Several papers about the applications of this problem have been presented in [28,37]. In Table 3, we compare the absolute errors of the present method for $M = 2, N = 1, \lambda = 0$ and $\gamma(x,t) = 1 - 0.5\exp(-xt)$ with methods in [1,15,36]. Also, Table 4 shows the absolute errors with various functions of $\gamma(x,t)$ with $h(t) = t, \cos(t)$, $\lambda = 1$ and employs two sentences of Legendre polynomials for expanded functions, including variable x and one sentence of Laguerre polynomials for expanded functions, including variable t. Moreover, CPU time (in seconds) is presented in Table 5. Figure 1 shows the absolute errors of approximate solutions obtained for $\gamma(x,t) = 1 - 0.3(1 + x^3)\exp(-t)$, $M = 2, N = 1$, $\lambda = 1$ and $h(t) = t$ with various intervals of t.

Table 3. Comparison of the absolute errors for $\gamma(x,t)$=$1 - 0.5\exp(-xt), t$=1 and λ=0, with methods in [1,15,36] for Example 3.

x_i	Present Method $M = 2, N = 1$	Method in [15] $N = 20$	Method in [36] $N = 100$	Method in [1] $M = N = 10$
0.1	4.84×10^{-18}	1.5629×10^{-4}	6.3759×10^{-5}	4.7781×10^{-15}
0.2	2.71×10^{-17}	1.4006×10^{-3}	4.9040×10^{-6}	1.1399×10^{-16}
0.3	6.46×10^{-17}	2.9751×10^{-3}	5.9837×10^{-5}	2.7608×10^{-16}
0.4	1.04×10^{-17}	4.2976×10^{-3}	7.7810×10^{-6}	7.0724×10^{-16}
0.5	1.31×10^{-16}	4.9721×10^{-3}	5.8089×10^{-5}	1.0486×10^{-17}
0.6	1.33×10^{-16}	4.8034×10^{-3}	8.2984×10^{-6}	2.3397×10^{-16}
0.7	1.09×10^{-16}	3.8152×10^{-3}	5.8931×10^{-5}	2.3096×10^{-16}
0.8	6.44×10^{-17}	2.2746×10^{-3}	5.9463×10^{-6}	8.4324×10^{-17}
0.9	1.86×10^{-17}	7.2075×10^{-4}	6.2975×10^{-5}	7.9527×10^{-17}
CPU	5.76×10^{-2}	-	-	-

Table 4. Absolute errors for various functions of $\gamma(x,t)$ and $h(t)$=$t, \cos(t)$ with $M = 2, N = 1, \lambda = 1$ of Example 3.

(x_i, t_i)	$\gamma(x,t)$=$1-0.5\exp(-xt)$	$\gamma(x,t)$=$1-\cos(x)\exp(-t)$	$\gamma(x,t)$=$0.25, 0.5, 1$
0	0	0	0
$(0.1, 0.1)$	4.30×10^{-18}	4.40×10^{-18}	2.21×10^{-18}
$(0.2, 0.2)$	1.97×10^{-17}	2.44×10^{-17}	1.18×10^{-17}
$(0.3, 0.3)$	4.82×10^{-17}	5.80×10^{-17}	2.70×10^{-17}
$(0.4, 0.4)$	8.01×10^{-17}	9.34×10^{-17}	4.13×10^{-17}
$(0.5, 0.5)$	1.04×10^{-16}	1.16×10^{-16}	4.76×10^{-17}
$(0.6, 0.6)$	1.12×10^{-16}	1.17×10^{-16}	4.16×10^{-17}
$(0.7, 0.7)$	1.00×10^{-16}	9.36×10^{-17}	2.37×10^{-17}
$(0.8, 0.8)$	7.01×10^{-17}	5.20×10^{-17}	8.07×10^{-19}
$(0.9, 0.9)$	3.18×10^{-17}	1.14×10^{-17}	1.37×10^{-17}
$(1, 1)$	5.87×10^{-39}	5.87×10^{-39}	1.87×10^{-39}

Table 5. CPU time for various functions of $\gamma(x,t)$ with $M=2, N=1, \lambda=1$ and $h(t)$=t of Example 3.

$\gamma(x,t)$	$1-0.5\exp(-xt)$	$1-\cos(x)\exp(-t)$	0.25	0.5	1
CPU	2.23×10^{-1}	2.40×10^{-1}	1.75×10^{-1}	1.72×10^{-1}	1.63×10^{-1}

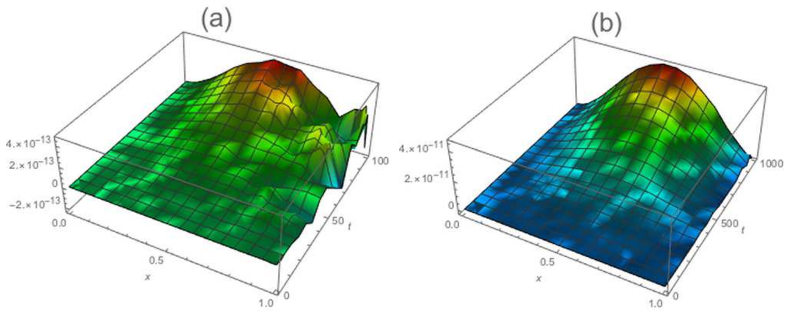

Figure 1. Absolute errors between the exact and approximate solutions for $\gamma(x,t)=1-0.3(1+x^3)\exp(-t)$, $M=2, N=1, \lambda=1$ and $h(t)=t$ with $t\in[0,100]$ (a) and $t\in[0,1000]$ (b) of Example 3.

Example 4. Consider

$$D_t^{\gamma(x,t)}u(x,t)+\frac{\partial^2 u}{\partial x^2}(x,t)+u(x,t)=g(x,t)+\int_0^1\int_0^{h(t)}\frac{u(\xi,\eta)}{(t-\eta)^{\frac{1}{2}}}d\eta d\xi$$

with the following initial condition $u(x,0)=0$, $0\le x\le 1$ and boundary conditions $u(0,t)=t^2$, $u(1,t)=t^2\exp(1)$, $t>0$. And also, $g(x,t)=\frac{\Gamma(3)}{\Gamma(3-\gamma(x,t))}t^{2-\gamma(x,t)}\exp(x)+2t^2\exp(x)-(\frac{16}{15}t^{\frac{5}{2}}-\frac{2}{15}(t-h(t))^{\frac{1}{2}}(3h(t)^2+4th(t)+8t^2))(\exp(1)-1)$. The exact solution of this example is $u(x,t)=t^2\exp(x)$. Table 6, presents the absolute errors for various values of $\gamma(x,t)$, M and N with $h(t)=t$. From Table 6, we can see clearly that the error gets smaller and smaller with increasing M. Due to Table 6 and Figure 2, it is clear that we achieve a good approximation of the exact solution by using a few terms of LLFs.

Figure 2. Errors between the exact and approximate solutions for $\gamma(x,t)=\frac{3+\sin(x)\cos(t)}{4}$ and $h(t)=t$ with $M=3, N=2$ (a) and $M=5, N=2$ (b) on the interval $[0,1]\times[0,1]$ of Example 4.

Table 6. Absolute errors with various values of $\gamma(x,t)$ and M with $h(t)=t$ and $N=2$ for Example 4.

(x_i,t_i)	$\gamma(x,t)=0.25$ $M=2$	$M=3$	$M=5$	$\gamma(x,t)=0.5$ $M=2$	$M=3$	$M=5$
$(0.1,0.1)$	$1.79e{-7}$	$1.12e{-9}$	7.64×10^{-10}	1.83×10^{-7}	4.37×10^{-8}	7.64×10^{-10}
$(0.3,0.3)$	$3.81e{-6}$	$3.17e{-7}$	1.45×10^{-8}	3.77×10^{-6}	5.91×10^{-7}	1.45×10^{-8}
$(0.5,0.5)$	$1.31e{-6}$	$4.89e{-7}$	4.50×10^{-8}	1.41×10^{-6}	9.78×10^{-7}	4.50×10^{-8}
$(0.7,0.7)$	$2.48e{-5}$	$1.76e{-6}$	6.99×10^{-8}	2.49×10^{-5}	2.26×10^{-6}	6.99×10^{-8}
$(0.9,0.9)$	$1.83e{-5}$	$1.10e{-7}$	4.69×10^{-8}	1.82×10^{-5}	1.16×10^{-7}	4.69×10^{-8}
(x_i,t_i)	$\gamma(x,t)=1$ $M=2$	$M=3$	$M=5$			
$(0.1,0.1)$	$1.67e{-7}$	$4.59e{-8}$	3.24×10^{-10}			
$(0.3,0.3)$	$3.83e{-6}$	$5.44e{-7}$	1.17×10^{-8}			
$(0.5,0.5)$	$2.48e{-5}$	$1.76e{-6}$	6.99×10^{-8}			
$(0.7,0.7)$	$2.49e{-5}$	$2.03e{-6}$	6.65×10^{-8}			
$(0.9,0.9)$	$1.82e{-5}$	$2.85e{-7}$	4.59×10^{-8}			

Example 5. Consider the VO-TF-PIDEs with weakly singular kernel

$$D_t^{\gamma(x,t)}u(x,t)+\frac{\partial u}{\partial x}(x,t)=g(x,t)+\int_0^x\int_0^{h(t)}\frac{u(\xi,\eta)}{(t-\eta)^{\frac{1}{2}}}d\eta d\xi,\qquad 0<\gamma(x,t)\le 1,$$

with the initial condition $u(x,0)=0$, $0\le x\le 1$ and boundary condition $u(0,t)=0$, $t>0$, and $g(x,t)=\frac{t^{1-\gamma(x,t)}}{\Gamma(2-\gamma(x,t))}\sin(x)+t\cos(x)+(\frac{4}{3}t^{\frac{3}{2}}-\frac{2}{3}(t-h(t))^{\frac{1}{2}}(2t+h(t)))(\cos(x)-1)$. The exact solution of this example is $u(x,t)=t\sin(x)$. In order to display the accuracy of the method, the absolute errors between the exact solution and numerical solutions for various choices of M,N and $\gamma(x,t)$ with $h(t)=t$ are shown in Table 7.

Table 7. The absolute errors for different values of M,N with $h(t)=t$ of Example 5.

(x_i,t_i)	$\gamma(x,t)=0.8+0.005\cos(xt)\sin(x)$ $M=2,N=1$	$M=4,N=1$	$\gamma(x,t)=0.5$ $M=2,N=1$	$M=4,N=1$
$(0,0)$	0	0	0	0
$(0.1,0.1)$	2.15×10^{-5}	6.71×10^{-8}	3.12×10^{-5}	8.50×10^{-8}
$(0.2,0.2)$	3.66×10^{-5}	5.56×10^{-8}	1.84×10^{-5}	9.24×10^{-8}
$(0.3,0.3)$	4.40×10^{-4}	3.44×10^{-8}	4.53×10^{-4}	8.24×10^{-8}
$(0.4,0.4)$	1.63×10^{-3}	1.00×10^{-7}	1.76×10^{-3}	1.59×10^{-7}
$(0.5,0.5)$	4.31×10^{-3}	1.75×10^{-7}	4.71×10^{-3}	2.50×10^{-7}
$(0.6,0.6)$	9.54×10^{-3}	1.48×10^{-7}	1.04×10^{-2}	2.42×10^{-7}
$(0.7,0.7)$	1.88×10^{-2}	1.05×10^{-7}	2.05×10^{-2}	2.19×10^{-7}
$(0.8,0.8)$	3.42×10^{-2}	3.36×10^{-7}	3.71×10^{-2}	4.80×10^{-7}
$(0.9,0.9)$	5.85×10^{-2}	7.37×10^{-7}	6.30×10^{-2}	9.18×10^{-7}
$(1,1)$	9.52×10^{-2}	8.58×10^{-7}	7.01×10^{-2}	6.83×10^{-7}

From Table 7, we can see clearly that the error gets smaller and smaller with increasing M for various functions of $\gamma(x,t)$. Table 8 illustrates $\|Res_{MN}\|^2_{2,w}$ for various values of $M,\gamma(x,t)$ with $h(t)=t$ and $N=1$. With regards to

Figure 3 and Table 7, it is seen that the approximate solutions converge to the exact solution.

Table 8. The error $\|Res_{MN}\|_{2,w}^2$ for different values of $M, N, \gamma(x,t)$ with $h(t) = t$ of Example5.

	$\gamma(x,t)=1$		$\gamma(x,t)=1-0.3\exp(-xt)$	
	$M=2, N=1$	$M=4, N=1$	$M=2, N=1$	$M=4, N=1$
$\|Res_{MN}\|_{2,w}^2$	1.3035×10^{-5}	2.5877×10^{-10}	8.2871×10^{-6}	1.3248×10^{-10}

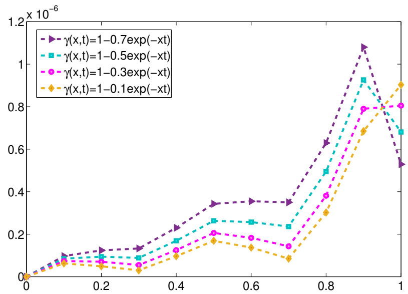

Figure 3. Absolute errors between the exact and approximate solutions for $t \in [0,1]$, $N = 1, M = 4$ with $h(t) = t$ and $x = 1$ of Example 5.

Example 6. Consider the VO-TF-PIDEs with weakly singular kernel

$$D_t^{\gamma(x,t)}u(x,t) + u(x,t) = g(x,t) + \int_0^x \int_0^t \frac{u_t(\xi,\eta)}{(x-\xi)^{\frac{1}{3}}}d\eta d\xi, \qquad 0 < \gamma(x,t) \le 1$$

with the initial condition $u(x,0) = \cos(x)$, $0 \le x \le 1$ and following boundary condition $u(0,t) = 1 + \sin(t)$, $t > 0$ where $g(x,t) = \cos(x) + \sin(t) + \cos(t) + \frac{3}{2}x^{\frac{2}{3}}\sin(t)$. The exact solution of this example, when $\gamma(x,t) = 1$ is $u(x,t) = \cos(x) + \sin(t)$. Table 9 shows the absolute errors for different values of N with $M = 1$ and $\gamma(x,t) = 1$. Due to the Table 9, by increasing the terms of Laguerre polynomials N the approximate solution converges to the exact solution. Figure 4 illustrates graphs of the approximate solution for various values of $\gamma(x,t)$ with $M = 1, N = 3$ and $x = 1$.

Example 7. As a final example, consider the VO-TF-PIDEs with weakly singular kernel

$$D_t^{\gamma(x,t)}u(x,t) = \frac{\partial u}{\partial x}(x,t) + \frac{\partial u}{\partial t}(x,t) + g(x,t) + \int_0^x \int_0^\rho \frac{u(\xi,\eta)}{(t-\eta)^{\frac{1}{2}}}d\eta d\xi, \qquad \rho > 0,$$

$0 < \gamma(x,t) \le 1$, with initial condition $u(x,0) = \cos(x)$, $0 \le x \le 1$ and boundary condition $u(0,t) = t^2 + 1$, $t > 0$ and $g(x,t) = \frac{2t^{2-\gamma(x,t)}}{\Gamma(3-\gamma(x,t))}\cos(x) - 2t\cos(x) +$

Table 9. Absolute errors for various values of N with $M = 1$ and $\gamma(x,t) = 1$ of Example 6.

(x_i, t_i)	$N = 1$	$N = 3$	$N = 5$
0	0	0	0
$(0.1, 0.1)$	5.80×10^{-3}	4.30×10^{-5}	1.08×10^{-7}
$(0.2, 0.2)$	8.24×10^{-3}	3.65×10^{-5}	6.58×10^{-8}
$(0.3, 0.3)$	8.24×10^{-3}	2.40×10^{-5}	6.96×10^{-8}
$(0.4, 0.4)$	6.68×10^{-3}	2.20×10^{-5}	9.50×10^{-8}
$(0.5, 0.5)$	4.42×10^{-3}	2.95×10^{-5}	1.13×10^{-7}
$(0.6, 0.6)$	2.27×10^{-3}	3.74×10^{-5}	1.39×10^{-7}
$(0.7, 0.7)$	1.02×10^{-3}	3.66×10^{-5}	1.86×10^{-7}
$(0.8, 0.8)$	1.37×10^{-3}	2.70×10^{-5}	2.26×10^{-7}
$(0.9, 0.9)$	3.97×10^{-3}	2.43×10^{-5}	2.37×10^{-7}
$(1, 1)$	9.41×10^{-3}	6.76×10^{-5}	4.06×10^{-7}

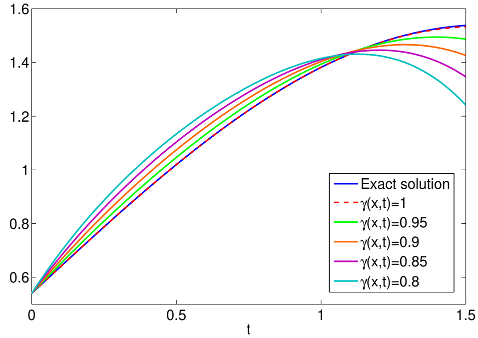

Figure 4. Approximate solutions for various values of $\gamma(x,t)$ with $M = 1, N = 3$ and $x = 1$ of Example 6.

$(t^2+1)\sin(x) - \int_0^x \int_0^\rho \frac{(\eta^2+1)\cos(\xi)}{(t-\eta)^{\frac{1}{2}}} d\eta d\xi$. The exact solution of this example is $u(x,t) = (t^2+1)\cos(x)$. The absolute errors for various choices of ρ, with $(x,t) \in [0,1] \times [0,10]$, $(x,t) \in [0,1] \times [0,50]$ and $M = 5, N = 2$ are plotted in Figure 5. These graphs illustrate that approximate solutions in various intervals have good accuracy.

8 Conclusions

This work introduces a new numerical approach for solving VO-TF-PIDEs with the weakly singular kernel. The method is based on expanding the derivation of the solution in terms of the LLFs and using the appropriate collocation points. The main objective is to use an integral pseudo-operational matrix of LLFs, which provides good conditions to receive the approximate solution with high accuracy. The advantage of the proposed method is that, despite defined time in an infinite interval, we achieved a good approximate solution. Also, satisfactory examples illustrate the validity and efficiency of the method.

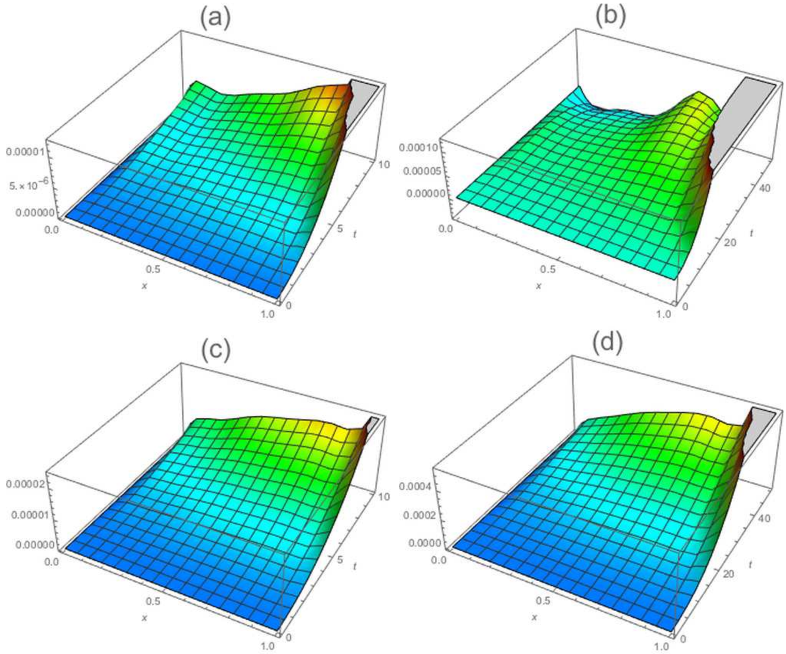

Figure 5. Absolute error between the exact and approximate solutions for $N = 2, M = 5$ and $\gamma(x,t) = 1 - 0.5x^2 \exp(-t)$ with a) $\rho = 50$ on the interval $[0,1] \times [0,10]$, b) $\rho = 50$ on the interval $[0,1] \times [0,50]$, c) $\rho = 100$ on the interval $[0,1] \times [0,10]$, d) $\rho = 100$ on the interval $[0,1] \times [0,50]$ of Example 7.

Acknowledgements

This work is supported by the National Elite Foundation and Alzahra University. We express our sincere thanks to the anonymous referees for valuable suggestions that improved the final manuscript.

References

[1] M.A. Abdelkawy, M.A. Zaky, A.H. Bhrawy and D. Baleanu. Numerical simulation of time variable fractional order mobile-immobile advection-dispersion model. *Romanian Reports in Physics*, **67**(3):773–791, 2015.

[2] A. Babaei, B.P. Moghaddam, S. Banihashemi and J.A.T. Machado. Numerical solution of variable-order fractional integro-partial differential equations via sinc collocation method based on single and double exponential transformations. *Communications in Nonlinear Science and Numerical Simulation*, **82**:104985, 2020. https://doi.org/10.1016/j.cnsns.2019.104985.

[3] D. Baleanu, R. Darzi and B. Agheli. New study of weakly singular kernel fractional fourth-order partial integro-differential equations based on the optimum q-homotopic analysis method. *Journal of Computational and Applied Mathematics*, **320**:193–201, 2017. https://doi.org/10.1016/j.cam.2017.01.032.

[4] Sh.S. Behzadi. The use of iterative methods to solve two-dimensional nonlinear Volterra-Fredholm integro-differential equations. *Communications in Numerical Analysis*, **2012**:1–20, 2012. https://doi.org/10.5899/2012/cna-00108.

[5] C. Canuto, M.Y. Hussaini, A. Quarteroni and T.A. Zang. *Spectral methods: fundamentals in single domains*. Springer Science & Business Media, 2007. https://doi.org/10.1007/978-3-540-30726-6.

[6] C.F.M Coimbra. Mechanics with variable-order differential operators. *Annalen der Physik*, **12**(11-12):692–703, 2003. https://doi.org/10.1002/andp.200310032.

[7] H. Dehestani, Y. Ordokhani and M. Razzaghi. Fractional-order Legendre–Laguerre functions and their applications in fractional partial differential equations. *Applied Mathematics and Computation*, **336**:433–453, 2018. https://doi.org/10.1016/j.amc.2018.05.017.

[8] H. Dehestani, Y. Ordokhani and M. Razzaghi. Application of the modified operational matrices in multiterm variable-order time-fractional partial differential equations. *Mathematical Methods in the Applied Sciences*, **42**(18):7296–7313, 2019. https://doi.org/10.1002/mma.5840.

[9] H. Dehestani, Y. Ordokhani and M. Razzaghi. Hybrid functions for numerical solution of fractional Fredholm-Volterra functional integro-differential equations with proportional delays. *International Journal of Numerical Modelling: Electronic Networks, Devices and Fields*, **32**(5):e2606, 2019. https://doi.org/10.1002/jnm.2606.

[10] M. Dehghan. Solution of a partial integro-differential equation arising from viscoelasticity. *International Journal of Computer Mathematics*, **83**(1):123–129, 2006. https://doi.org/10.1080/00207160500069847.

[11] G. Diaz and C.F.M Coimbra. Nonlinear dynamics and control of a variable order oscillator with application to the van der Pol equation. *Nonlinear Dynamics*, **56**(1):145–157, 2009. https://doi.org/10.1007/s11071-008-9385-8.

[12] G. Fairweather. Spline collocation methods for a class of hyperbolic partial integro-differential equations. *SIAM journal on numerical analysis*, **31**(2):444–460, 1994. https://doi.org/10.1137/0731024.

[13] L. Hörmander. *The analysis of linear partial differential operators I: Distribution theory and Fourier analysis*. Springer, 2015. https://doi.org/10.1007/978-3-642-61497-2.

[14] D. Ingman and J. Suzdalnitsky. Control of damping oscillations by fractional differential operator with time-dependent order. *Computer Methods in Applied Mechanics and Engineering*, **193**(52):5585–5595, 2004. https://doi.org/10.1016/j.cma.2004.06.029.

[15] W. Jiang and N. Liu. A numerical method for solving the time variable fractional order mobile–immobile advection–dispersion model. *Applied Numerical Mathematics*, **119**:18–32, 2017. https://doi.org/10.1016/j.apnum.2017.03.014.

[16] J.B. Keller and W.E. Olmstead. Temperature of a nonlinearly radiating semi-infinite solid. *Quarterly of Applied Mathematics*, **29**(4):559–566, 1972. https://doi.org/10.1090/qam/403430.

[17] R. Lin, F. Liu, V. Anh and I. Turner. Stability and convergence of a new explicit finite-difference approximation for the variable-order nonlinear fractional diffusion equation. *Applied Mathematics and Computation*, **212**(2):435–445, 2009. https://doi.org/10.1016/j.amc.2009.02.047.

[18] P. Linz. *Analytical and numerical methods for Volterra equations.* Society for Industrial and Applied Mathematics, 1985. https://doi.org/10.1137/1.9781611970852.

[19] W. McLean, I.H. Sloan and V. Thomée. Time discretization via Laplace transformation of an integro-differential equation of parabolic type. *Numerische Mathematik*, **102**(3):497–522, 2006. https://doi.org/10.1007/s00211-005-0657-7.

[20] B.P. Moghaddam and J.A.T. Machado. A computational approach for the solution of a class of variable-order fractional integro-differential equations with weakly singular kernels. *Fractional Calculus and Applied Analysis*, **20**(4):1023–1042, 2017. https://doi.org/10.1515/fca-2017-0053.

[21] B.P. Moghaddam and J.A.T. Machado. Time analysis of forced variable-order fractional Van der Pol oscillator. *The European Physical Journal Special Topics*, **226**(16):3803–3810, 2017. https://doi.org/10.1140/epjst/e2018-00019-7.

[22] B.P. Moghaddam, J.A.T. Machado and H. Behforooz. An integro quadratic spline approach for a class of variable-order fractional initial value problems. *Chaos, Solitons & Fractals*, **102**:354–360, 2017. https://doi.org/10.1016/j.chaos.2017.03.065.

[23] B.P. Moghaddam and J.T. Machado. A stable three-level explicit spline finite difference scheme for a class of nonlinear time variable order fractional partial differential equations. *Computers & Mathematics with Applications*, **73**(6):1262–1269, 2017. https://doi.org/10.1016/j.camwa.2016.07.010.

[24] P. Muthukumar and B. Ganesh Priya. Numerical solution of fractional delay differential equation by shifted Jacobi polynomials. *International Journal of Computer Mathematics*, **94**(3):471–492, 2017. https://doi.org/10.1080/00207160.2015.1114610.

[25] S. Nemati, P.M. Lima and Y. Ordokhani. Numerical solution of a class of two-dimensional nonlinear Volterra integral equations using Legendre polynomials. *Journal of Computational and Applied Mathematics*, **242**:53–69, 2013. https://doi.org/10.1016/j.cam.2012.10.021.

[26] V.K. Patel, S. Singh, V.K. Singh and E. Tohidi. Two dimensional wavelets collocation scheme for linear and nonlinear Volterra weakly singular partial integro-differential equations. *International Journal of Applied and Computational Mathematics*, **4**(5):132, 2018. https://doi.org/10.1007/s40819-018-0560-4.

[27] L.E.S. Ramirez and C.F.M. Coimbra. On the variable order dynamics of the nonlinear wake caused by a sedimenting particle. *Physica D: Nonlinear Phenomena*, **240**(13):1111–1118, 2011. https://doi.org/10.1016/j.physd.2011.04.001.

[28] R. Schumer, D.A. Benson, M.M. Meerschaert and B. Baeumer. Fractal mobile/immobile solute transport. *Water Resources Research*, **39**(10), 2003. https://doi.org/10.1029/2003WR002141.

[29] H. Sheng, H. Sun, Y.Q. Chen and T.S. Qiu. Synthesis of multifractional Gaussian noises based on variable-order fractional operators. *Signal Processing*, **91**(7):1645–1650, 2011. https://doi.org/10.1016/j.sigpro.2011.01.010.

[30] S. Singh, V.K. Patel and V.K. Singh. Operational matrix approach for the solution of partial integro-differential equation. *Applied Mathematics and Computation*, **283**:195–207, 2016. https://doi.org/10.1016/j.amc.2016.02.036.

[31] S. Singh, V.K. Patel and V.K. Singh. Convergence rate of collocation method based on wavelet for nonlinear weakly singular partial integro-differential equation arising from viscoelasticity. *Numerical Methods for Partial Differential Equations*, **34**(5):1781–1798, 2018. https://doi.org/10.1002/num.22245.

[32] S. Singh, V.K. Patel, V.K. Singh and E. Tohidi. Numerical solution of nonlinear weakly singular partial integro-differential equation via operational matrices. *Applied Mathematics and Computation*, **298**:310–321, 2017. https://doi.org/10.1016/j.amc.2016.11.012.

[33] C.M. Soon, C.F.M. Coimbra and M.H. Kobayashi. The variable viscoelasticity oscillator. *Annalen der Physik*, **14**(6):378–389, 2005. https://doi.org/10.1002/andp.200410140.

[34] T. Tang. A finite difference scheme for partial integro-differential equations with a weakly singular kernel. *Applied Numerical Mathematics*, **11**(4):309–319, 1993. https://doi.org/10.1016/0168-9274(93)90012-G.

[35] A.-M. Wazwaz. A reliable treatment for mixed Volterra–Fredholm integral equations. *Applied Mathematics and Computation*, **127**(2-3):405–414, 2002. https://doi.org/10.1016/S0096-3003(01)00020-0.

[36] H. Zhang, F. Liu, M.S. Phanikumar and M.M. Meerschaert. A novel numerical method for the time variable fractional order mobile–immobile advection–dispersion model. *Computers & Mathematics with Applications*, **66**(5):693–701, 2013. https://doi.org/10.1016/j.camwa.2013.01.031.

[37] Y. Zhang, D.A. Benson and D.M. Reeves. Time and space nonlocalities underlying fractional-derivative models: Distinction and literature review of field applications. *Advances in Water Resources*, **32**(4):561–581, 2009. https://doi.org/10.1016/j.advwatres.2009.01.008.